JOURNAL OF MATERIALS SCIENCE 29 (1994) 1501–1506

Sintering and mechanical properties of β-wollastonite

T. ENDO, S. SUGIURA, M. SAKAMAKI, H. TAKIZAWA, M. SHIMADA
Department of Molecular Chemistry and Engineering, Faculty of Engineering, Tohoku University, Aoba, Aoba-ku, Sendai City, Miyagi 980, Japan

Detailed microstructural studies have been carried out on porous β-wollastonite ($CaSiO_3$) ceramics with 40–60% of the theoretical density. Xonotlite ($Ca_6Si_6O_{17}(OH)_2$) was used as starting material, and the reaction and sintering behaviour were systematically examined in the range 800–1200 °C in air. Analysis of the mechanical properties showed that the strength degradation of β-wollastonite ceramics was certainly induced by the change of microstructure. Isothermal annealing at 1100 °C, however, did not preferentially affect the microstructure or the mechanical properties of sintered β-wollastonite. These observations lead to the conclusion that the measured bending strength and Vickers hardness of porous β-wollastonite ceramics can be substantially modified and improved by controlling the microstructure, in particular due to the shape of randomly oriented grains in the matrix.

1. Introduction

Studies of calcium silicates, especially wollastonite, β-$CaSiO_3$, have attracted attention in recent years. This arises from the fact that calcium silicate ceramics can be used for many building construction and engineering applications because of their improved friction and wear behaviour, enhanced fracture toughness, thermal shock resistance and machinability. The preparation of fine $CaSiO_3$ powders has been established by a coprecipitation method [1], the recrystallization via the heating process just at or below the temperature of incongruent melting [2], etc. More recently, comprehensive studies on polytypism and the stacking disorder have been carried out in a family of $CaSiO_3$ [3–5]. The results were also compared and contrasted with geological and mineralogical studies, leading to the conclusion that the morphology of crystalline $CaSiO_3$ reflects upon the configuration of silicate chains, i.e. a variable stacking sequence of $[SiO_3]$ chains within the crystal structure.

In the system $CaO–SiO_2–H_2O$, several previous publications have shown that the hydrated products formed at various stages of the thermal dehydration, and brought about any temperature-induced topotactical changes in these products in relation to the original calcium silicate hydrates, e.g. xonotlite, tobermorite, etc. [6–8]. Most of the starting powders were acicular or fibrous, and were readily densified without any sintering additives. This verified that fibrous xonotlite powders coagulated spontaneously on heating above 800 °C, corresponding to the temperature dehydrated and transformed completely into $CaSiO_3$.

In the present paper, it will be shown that the mechanical properties of β-$CaSiO_3$ compacts with different microstructures are explained as resulting from thermal dehydration and topotactical changes of xonotlite at elevated temperatures during the densification process.

2. Experimental procedure

Xonotlite ($Ca_6Si_6O_{17}(OH)_2$) was used in powder or slurry as starting material which was supplied by Onoda Cement Co. Ltd. After filtrating and drying the slurries, the thermal behaviour was characterized by thermogravimetric differential thermal analysis (TG-DTA) in air. The resulting powders were identified by X-ray powder diffraction (XRD) with CuK_α filtered by nickel. The starting powders were uniaxially pressed at 50 MPa to form platy specimens ($5 \times 15 \times 33\ mm^3$) prior to cold isostatic pressing at 200 MPa. The specimens were sintered at temperatures ranging from 800 to 1200 °C (heating rate = 1.5 °C min^{-1}) for 1 to 120 h in air. The sintered specimens were annealed at 1100 °C for 24 h in air and quenched to room temperature. The densities of recovered specimens were calculated from measurements of their weight and dimensions. The phase identification of the specimens was carried out by XRD. Platy specimens were cut into rectangular coupons, $4 \times 5 \times 15\ mm^3$, and polished. The three-point bending strength and Vickers hardness were measured at room temperature. For measuring bending strength, 10 or more test specimens with dimensions of $4 \times 5 \times 13\ mm^3$ were tested. The span was 10 mm and the cross-head speed 0.5 mm min^{-1}. The Vickers indenter was impressed under the desired load for 15 s on the polished specimen surface. Microstructural observations were carried out with an ABT-55 type scanning electron microscope (SEM).

3. Results and discussion

3.1. Dehydration of xonotlite

A SEM photograph of fine xonotlite powders obtained from the slurries is shown in Fig. 1. Many tiny, acicular particles appear to be twisted and agglomerated together to make a pierced cocoon shape. Fig. 2 shows the TG-DTA data of xonotlite powder. On

0022–2461

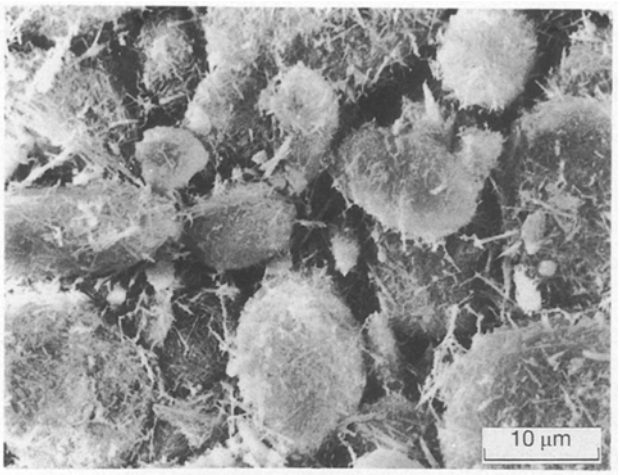

Figure 1 SEM photograph of xonotlite powders as starting material.

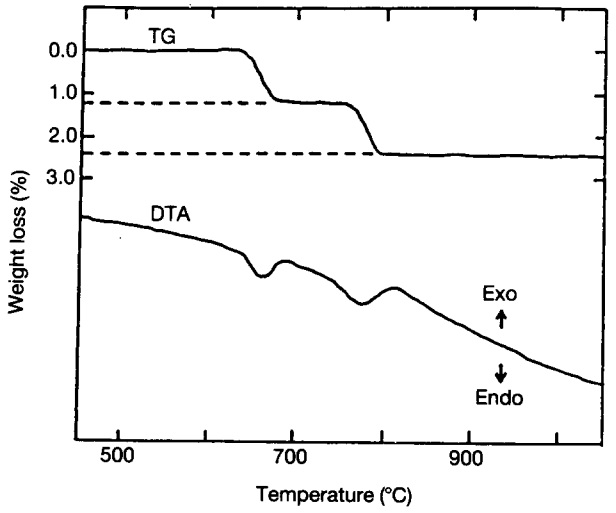

Figure 2 TG-DTA curves of xonotlite.

heating above 800 °C in air, xonotlite was completely transformed into β-wollastonite, β-$CaSiO_3$. The thermal change was obviously brought about by two-step weight loss, corresponding to the dehydration of xonotlite, as shown in Fig. 2. This profile is in line with the fact that xonotlite has two kinds of structural OH group [7]. However, the formation of precursor, formulated as $Ca_{12}Si_{12}O_{35}$ $(OH)_2$ was presumptive, because no structural evidence is available. All attempts to obtain such a precursor failed despite variations in the experimental procedures on calcinating at 700–800 °C in air. Furthermore, it was found that $Ca_{12}Si_{12}O_{35}(OH)_2$ was preferably recovered to xonotlite in air due to its vigorous hygroscopic characteristics.

3.2. Sintering of wollastonite

Sintering of β-wollastonite was carried out by use of the xonotlite compacts moulded at 200 MPa. Fig. 3 shows the relative density of recovered compacts as a function of sintering temperature for 24 h in air. The particle-packing density of xonotlite was evaluated to

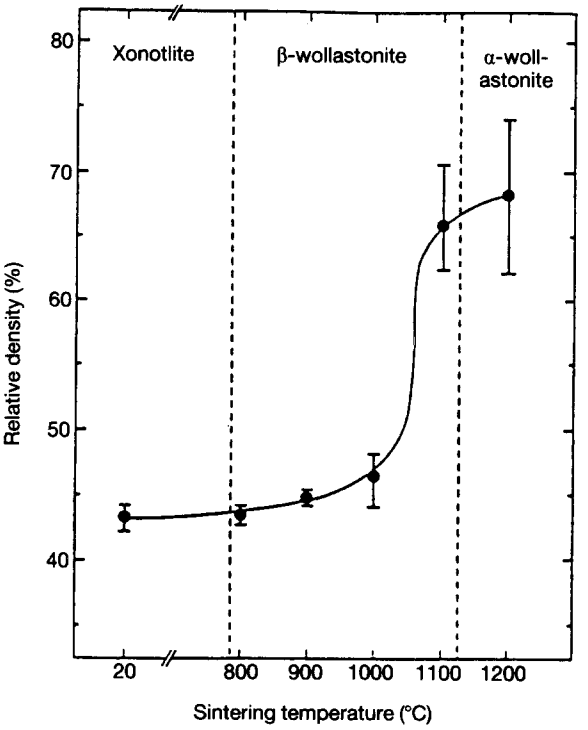

Figure 3 Relative density of sintered specimens as a function of sintering temperature for 24 h in air. Theoretical density of xonotlite and β-wollastonite are 2.83 and 2.91 g cm^{-3}, respectively.

be about 43% of the theoretical density. The relative density was hardly changed after calcinating at about 800 °C. This suggested that the dehydration of xonotlite would be intrinsically topotactic. The XRD results indicated that the sintered bodies, on calcinating in the temperature range 800–1130 °C, consisted of a phase identified only as β-wollastonite. The relative density of each β-wollastonite compact was independent of the sintering time of 1–120 h. Nevertheless, a large difference in relative density was found between the specimens of β-wollastonite sintered at 1000 and 1100 °C.

Fig. 4 shows SEM photographs of the fracture surfaces of the β-wollastonite compacts sintered at 800, 900, 1000 and 1100 °C, respectively. As the bulk and surface diffusions thermally progressed, the individual particles were moderately transformed from fibrous into platelet shapes. On heating at 900 °C, needle-like particles were packed into a bundle, and continued to grow. Beyond 1000 °C, platelet particles were observed in the microstructure of sintered bodies. Above 1100 °C, spaces between particles and occasionally larger voids resulting from the bridging of particles drastically collapsed with the large shrinkage of specimens. That is, the more rapid elimination of micropores was abruptly caused at or near the grain boundaries on heating. The densification profile of β-wollastonite was understood on the basis of observation, as shown in Fig. 4d, in which the fracture was enhanced at a different part from the particle interface.

The effect of absorbed water on the sintering process, especially the sintering rate, was investigated at 0.02, 0.2 and 0.3 atm of water vapour pressure (p_{H_2O}). Fig. 5 shows the relative density of β-wollastonite sintered at both 800 and 1000 °C as a function of

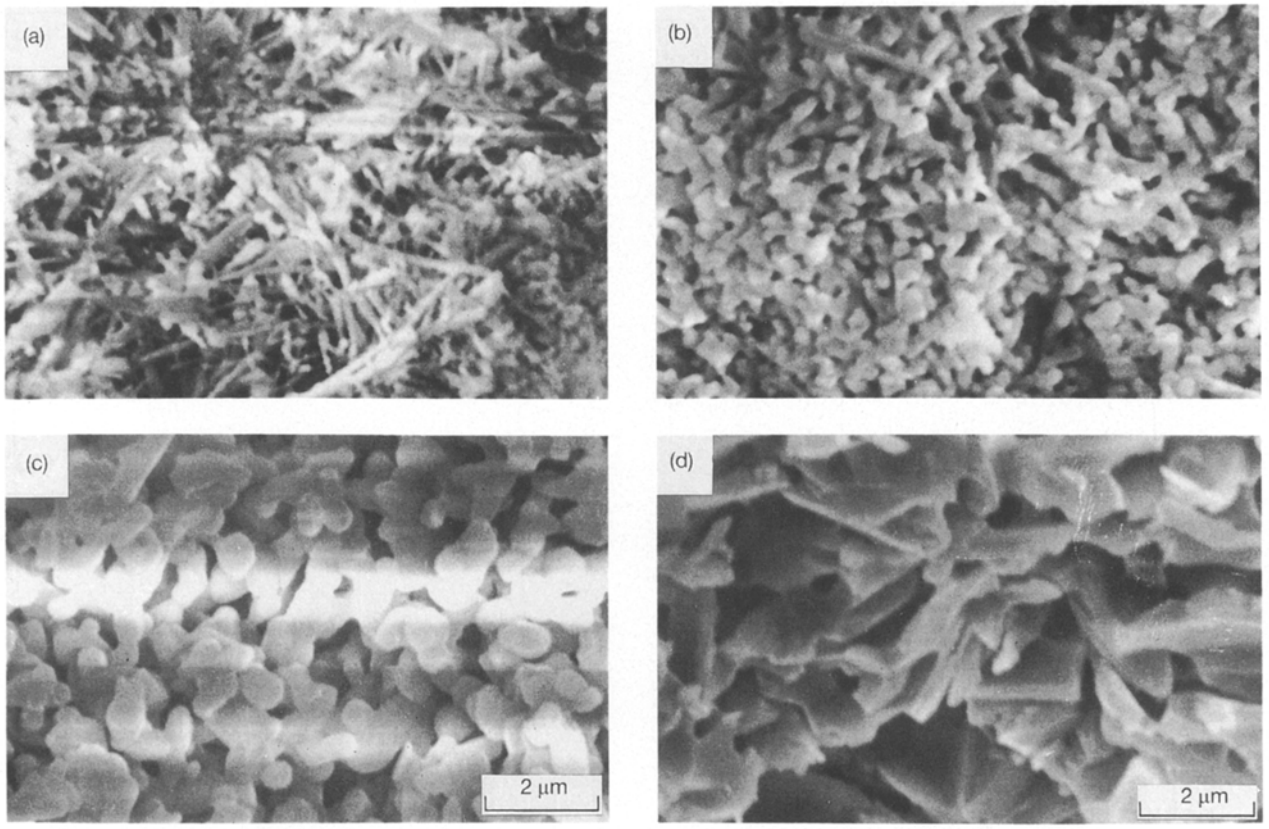

Figure 4 SEM photographs of the fracture surface of β-wollastonite compacts sintered at (a) 800, (b) 900, (c) 1000 and (d) 1100 °C for 24 h.

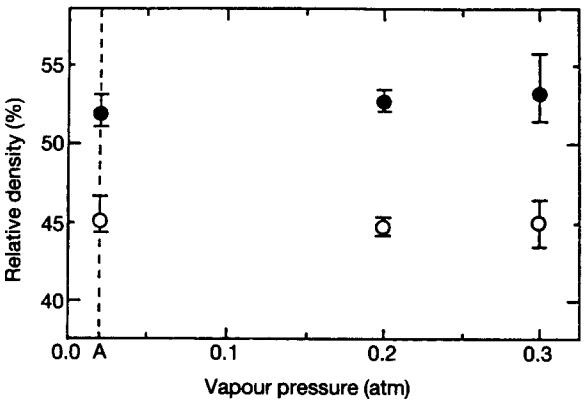

Figure 5 Relative density of β-wollastonite compacts sintered at (○) 800 and (●) 1000 °C for 24 h as a function of water vapour pressure. A is the point of water vapour pressure at 17 °C in air.

p_{H_2O}. This figure shows that the relative density was little affected by p_{H_2O}. There were no remarkable variations (such as etching near the grain boundary) in the resulting microstructure of sintered bodies, despite leaching of porous specimens in the high-temperature stream of water vapour.

3.3. Mechanical properties of sintered wollastonite

Fig. 6 shows the relationship between the bending strength of sintered body and sintering temperature for 24 h in air. As seen in this figure, the largest bending strength value is obtained at 1100 °C, corresponding to the sintering temperature at which the micropores were eliminated thoroughly from the particle boundaries. Above 1150 °C, the bending strength was considerably degraded by the transformation of β-phase into α-phase of wollastonite.

Fig. 7 shows the Weibull plots for the bending strength of sintered wollastonite. The Weibull modulus is determined by the slope shown in this figure. The observed values of specimens sintered at 800 and 1200 °C were relatively higher than those of the other specimens. This seemed to be closely related to the microstructure, especially the distribution of the pores and the shape of particles formed in the sintered bodies, as discussed above. The uniformity of the porous specimens was likely to fade during the growth process of each particle.

Fig. 8 shows the Vickers hardness of sintered β-wollastonite as a function of the sintering temperature. In the β-wollastonite specimen sintered at 1200 °C, a higher Vickers hardness value was obtained, whereas the lower value of the bending strength was obtained on comparing with the other compacts. This fact led to the conclusion that the Vickers hardness strongly depended on the relative density of the sintered body.

3.4. Isothermal annealing of sintered wollastonite

Four kinds of β-wollastonite sintered bodies, which were fabricated at 800, 900, 1000 and 1100 °C, were annealed at 1100 °C for 24 h in order to evaluate the thermal behaviour of β-wollastonite sintered body. Each relative density of the resulting specimens is represented in region II of Fig. 9. The drastic changes

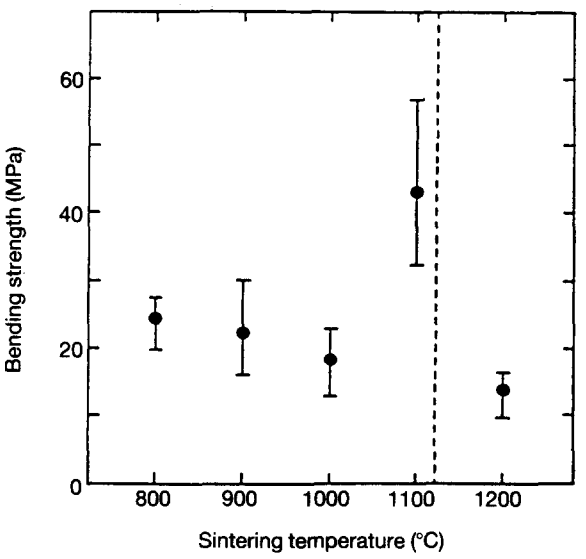

Figure 6 Bending strength of β-wollastonite compacts as a function of sintering temperature for 24 h in air.

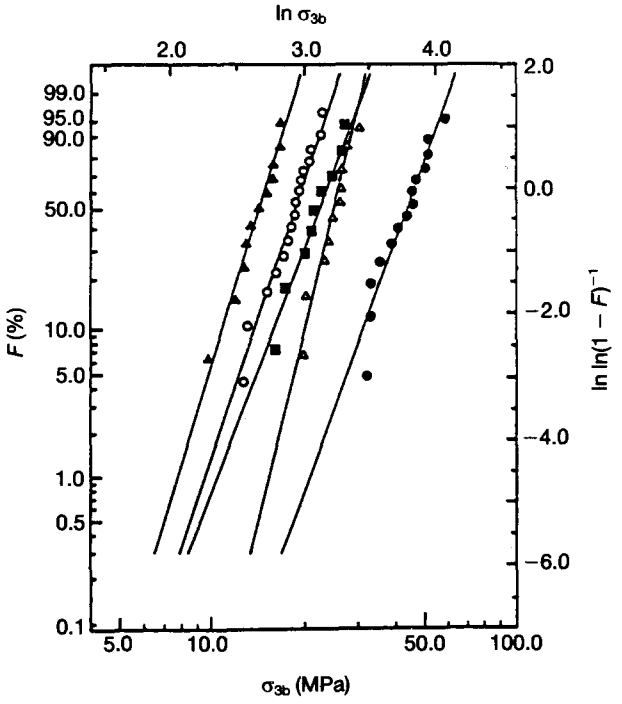

Figure 7 Weibull plots of bending strength (σ_{3b}) of β-wollastonite compacts. △, 800 °C (24 h), $m = 9.0$; ■, 900 °C (24 h), $m = 5.6$; ○, 1000° C (24 h), $m = 6.4$; ● 1100 °C (24 h), $m = 5.8$; ▲, 1200 °C (24 h), $m = 7.0$.

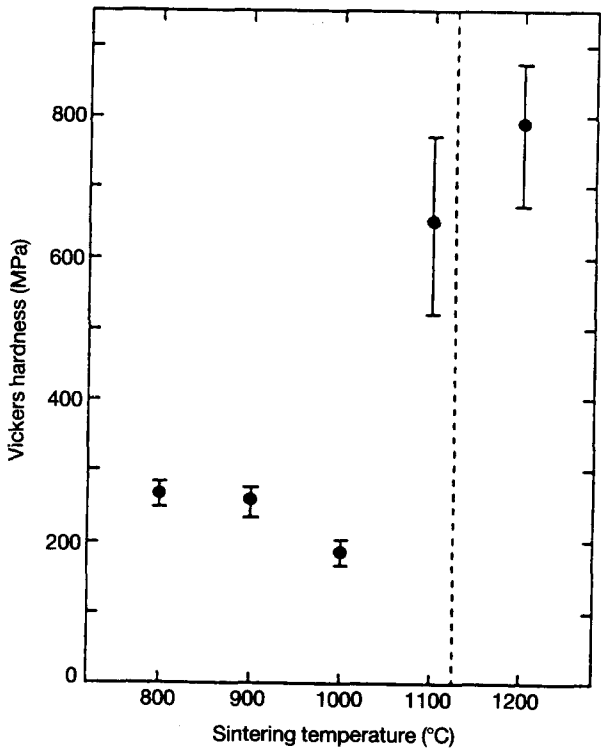

Figure 8 Vickers hardness of β-wollastonite compacts as a function of sintering temperature for 24 h in air.

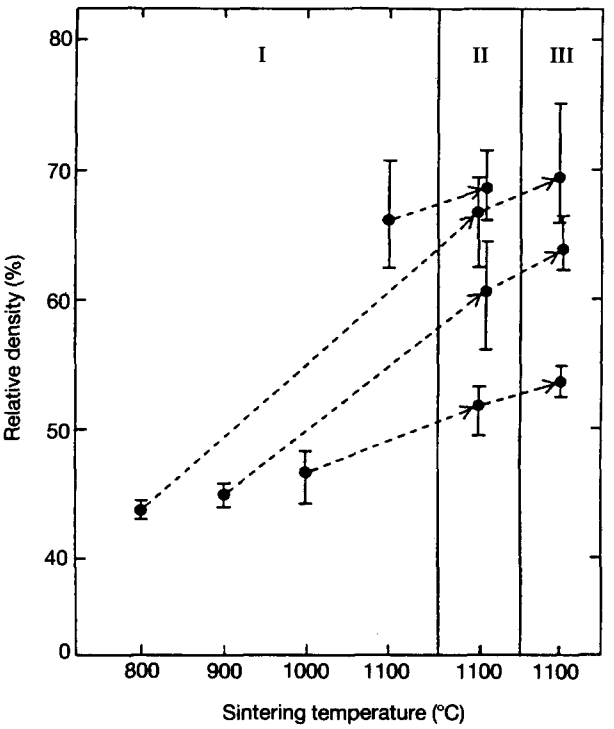

Figure 9 Relative density of β-wollastonite compacts as a function of sintering temperature. I, first sintering at each temperature for 24 h; II, second sintering at 1100 °C for 24 h; III, third sintering at 1100 °C for 24 h.

in relative density were observed only for the specimens sintered at 800 and 900 °C. The higher the sintering temperature, the less the change in relative density. Successively, the recovered specimens were annealed at 1100 °C for 24 h. The moderate densification of each compact was considered to advance with annealing time. However, the final density of the compact was governed by the initial sintering temperature, as shown in region III of Fig. 9. Figs 10 and 11 show the results of bending strength and Vickers hardness for the recovered specimens as a function of sintering temperature and annealing conditions. As a result, it was verified that the changes in bending strength and Vickers hardness responded well to the improvement in relative density.

Fig. 12 shows SEM photographs of β-wollastonite compacts annealed at 1100 °C for 24 h. This observation would suggest that the microstructure of each annealed compact was changed efficiently by controlling the initial sintering temperature.

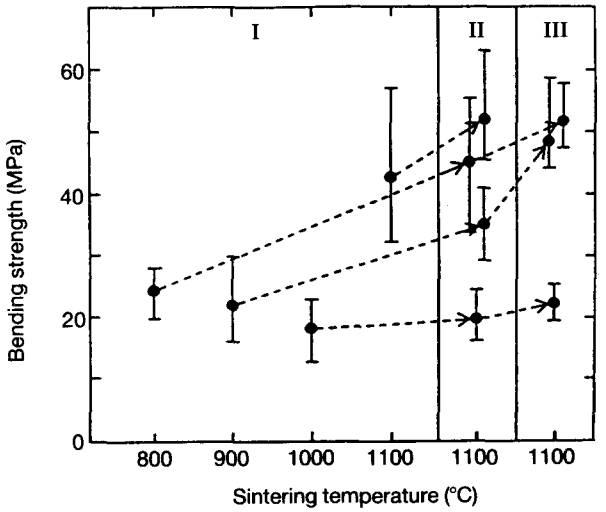

Figure 10 Bending strength of β-wollastonite compacts as a function of sintering temperature.

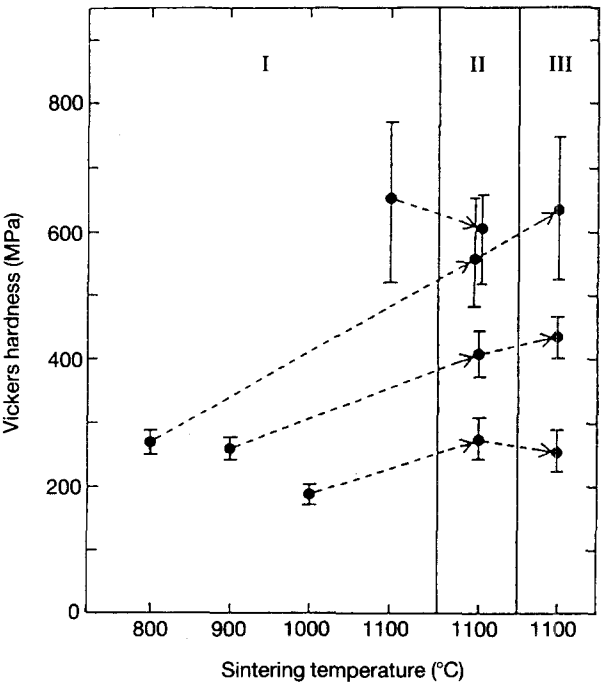

Figure 11 Vickers hardness of β-wollastonite compacts as a function of sintering temperature.

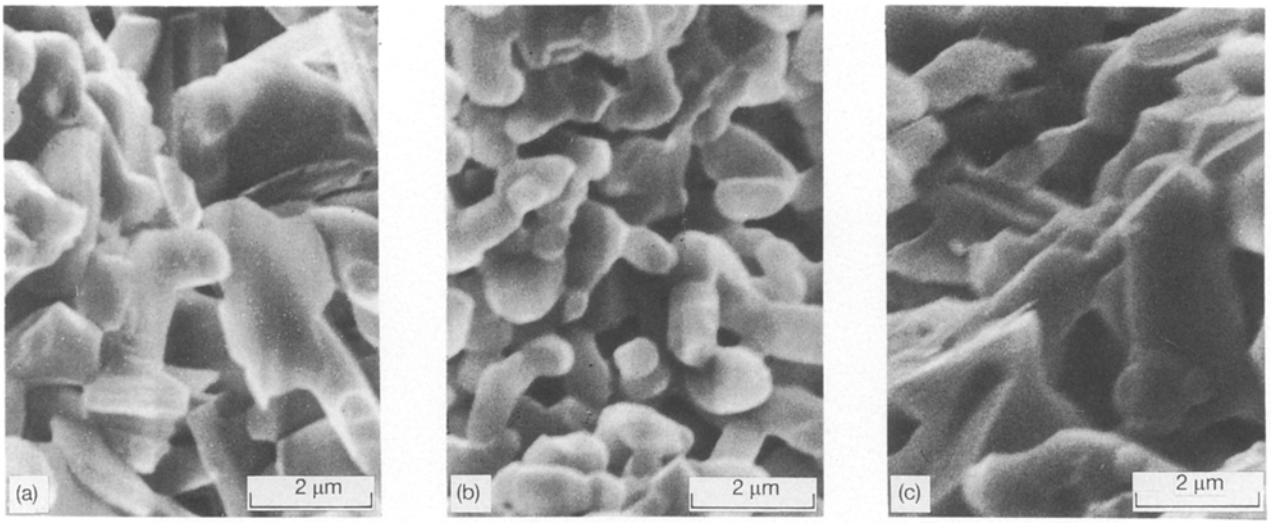

Figure 12 SEM photographs showing the thermal changes of β-wollastonite compacts sintered at (a) 800, (b) 1000 and (c) 1100 °C for 24 h. (a) Needle-like; (b) granular and (c) platelet grains.

4. Conclusions

1. On heating at 800 °C, xonotlite used in the present experiment dissociated step-wise and released two kinds of structural OH groups prior to the formation of β-wollastonite.

2. β-wollastonite was well sintered through the self-diffusion process in the range 800–1100 °C, but was almost independent of the sintering time within 120 h.

3. Individual β-wollastonite particles were obviously changed in shape such as fibrous, granular and platy ones at 800, 1000 and 1100 °C, respectively.

4. Dehydration and changes in relative density and microstructure were hardly affected by the water vapour pressure up to 0.3 atm.

5. High values of bending strength and Vickers hardness were only obtained from the porous β-wollastonite sintered at about 1100 °C. It was expected that the mechanical properties of a β-wollastonite sintered body would be closely related to the formation and consolidation of platy particles with a size uniformity in the sintered body.

6. By annealing the sintered compacts at 1100 °C for 24 h, the relative densities and mechanical properties of annealed specimens changed drastically. However, the microstructure of annealed specimens was eventually subject to the initial microstructure.

Acknowledgements

The authors thank the Onoda Cements Co., Ltd for supplying various kinds of starting materials. One of the authors (T.E.) would like to thank

Dr K. Tsukiyama (Onoda Cement Co., Ltd), Dr K. Kunugida and Mr Y. Isu (Onoda ALC Co., Ltd) for fruitful suggestions and discussion.

References

1. S. HAYASHI, K. OKADA and N. OTSUKA, *J. Ceram. Soc. Jpn.* **99** (1991) 1224.
2. H. IMAI, T.TAKEUCHI and Y. FUJIKI, "Kobutsu Kougaku" (Asakura Book Co Ltd, Tokyo, Japan, 1979) p. 111.
3. J. L. HUTCHISON and A. C. McLAREN, *Contrib. Mineral.* **55** (1976) 303.
4. F. J. TROJER, *Z. Krist.*, **130** (1969) S. 185.
5. D. A. JEFFERSON, N. J. PUGH, M. ALARIO-FRANCO, L. G. MALLINSON, G. R. MILLWARD and J. M. THOMAS, *Acta. Cryst.* **A36** (1980) 1058.
6. F. P. GLASSER, E. E. LACHOWSKI and D. E. MACPHEE, *J. Amer. Ceram. Soc.* **70** (1987) 481.
7. K. KUBO, T. MIZUNO, G. YAMGUCHI and H. HAYASHI, *J. Ceram. Soc. Jpn.* **82** (1974) 569.
8. D. R. MOOREHEAD and R. E. McCARTNEY, *J. Amer. Ceram. Sco.* **48** (1965) 565.

Received 16 September 1992
and accepted 27 September 1993